MELILITE FROM SYNTHETIC AND NATURAL TYPE B CAIS: SIMILARITIES AND DIFFERENCES. R. A. Mendybaev[1,2], A. M. Davis[1,2,3], F. M. Richter[1,2], and D. S. Ebel[4]. [1]Department of the Geophysical Sciences, [2]Chicago Center for Cosmochemistry, [3]Enrico Fermi Institute, University of Chicago, Chicago, IL, 60637 (ramendyb@uchicago.edu); [4]Department of Earth and Planetary Sciences, American Museum of Natural History, New York, NY 10024.

Introduction: Type B CAIs, composed mainly of melilite, fassaite, anorthite and spinel, represent one of the major types of coarse-grained CAIs found in carbonaceous chondrites. The uniform distribution of minerals observed in natural Type B2 CAIs was successfully reproduced in the laboratory [1] by slow cooling of partially molten droplets of CAIB composition under oxidizing conditions. Similar experiments under extremely reducing conditions (~log f_{O_2}<IW–6) result in formation of a melilite mantle [2], which is a characteristic feature of Type B1 CAIs. We argued [2, 3] that formation of the melilite mantle is caused by fast, compared to diffusion, evaporation of Mg and Si, which results in formation of Mg- and Si-depleted surface layer from which gehlenitic melilite crystallizes first. As the droplet continues to cool, åkermanitic melilite along with pyroxene and anorthite will form.

The composition of melilite and its zoning pattern sometimes are considered as an indicator of the conditions at which the CAIs have been formed. The zoning patterns obtained from a single profile through a melilite crystal, however, can be misleading, because even simple one-stage cooling of CMAS liquids results complexly zoned melilite [2]. The actual zoning pattern, which can be easily missed if only one profile is taken, can be obtained by detailed quantitative X-ray mapping.

In this work we present our results of a comparative study of melilite from natural Type B CAIs and their synthetic analogs.

Samples and Analytical Methods: We examined three Type B1 CAIs (USNM 3535-1, AMNH 4308-ALCAI1-sB1, and SH-1 from the Leoville, Allende and Sahara 98044 CV3 chondrites, respectively) and AL3529-26 from Allende, which has a layered texture with a thin melilite-enriched rim. The sections have been studied using a JEOL JSM-5800LV scanning electron microscope (SEM) with an Oxford/Link ISIS-300 X-ray microanalysis system. Detailed Åk maps of melilite were made from quantitative analysis of each spot in a grid of 256×192 spots.

Results: Leo3535 and SH-1 are typical Type B1 inclusions composed of melilite, spinel, pyroxene and anorthite. Both inclusions have a well-developed melilite mantle. ALCAI1-sB1 is a fragment cut from a large inclusion from Allende CV3 chondrite previously analyzed using a high spatial resolution microtomography technique [4]. Unlike in Leo3535 and SH-1, the melilite mantle of ALCAI1-sB1 is not continuous and covers about 80% of the edge of the inclusion.

Leo3535 is a spherical inclusion (9×6.5 mm) very similar to USNM 3537-2 described in [5]. The melilite mantle (~0.3–1.0 mm thick) is depleted in spinel compared to the interior of the inclusion. In general, melilite in the outermost part of the mantle is very gehlenitic (as low as $Åk_6$) and it becomes more åkermanitic ($Åk_{55–60}$) toward the central parts (Fig. 1). Note the sharp differences in composition of melilite from mantle and interior of the sample. A histogram of melilite composition in the mantle is characterized by distinct peaks at $Åk_{22}$, $Åk_{28–30}$, $Åk_{46}$, and $Åk_{55–57}$. Pockets of very åkermanitic melilite (up to $Åk_{75}$) can be found quite often within the mostly gehlenitic mantles. Melilite outside of the mantle is very åkermanitic (Fig. 1) with composition ranging from ~$Åk_{55}$ to ~$Åk_{75}$ with a peak at ~$Åk_{70}$.

Melilite in ALCAI1-sB1 appears as: (1) irregularly shaped crystals (some free of spinel) in melilite mantle; (2) melilite laths up to 2.5 mm long and 0.5 mm wide compactly located at one part of the inclusion; and (3) elongated (up to 0.5 mm) and/or irregularly shaped crystals in the interior of the inclusion. Melilite from the mantle and large laths ranges in composition from ~$Åk_{15}$ to $Åk_{65}$ peaking at ~$Åk_{37–40}$. The zoning pattern of the mantle melilite is quite complex: in some crystals Åk content first decreases from ~$Åk_{40–45}$ at the edge to $Åk_{30–35}$ toward the interior and then increases again to $Åk_{45–50}$, while other crystals are either asymmetrically zoned from ~$Åk_{30}$ at the edge to ~$Åk_{40}$ toward the interior, or unzoned with $Åk_{30–35}$ or exhibit very irregular zoning patterns. Melilite crystals forming large laths are generally normally zoned with ~$Åk_{50}$ at the edges and ~$Åk_{35}$ in the center (Fig. 2). But a detailed picture is quite complicated: profiles taken through the same grain might show normal, asymmetric normal, unzoned and even a reversed zoning patterns in the central parts of the crystal. In addition, in the central parts of the crystal there are small areas with Åk as low as $Åk_{10}$, which presumably represent relicts that survived all melting events. Small melilite crystals from the central parts of the inclusion are very åkermanitic with Åk varying from ~$Åk_{45}$ to $Åk_{78}$ with a peak at ~$Åk_{68–72}$.

Although SH-1 has very well-developed melilite mantle, composition of melilite in the mantle and core is essentially the same: $Åk_5$ to $Åk_{76}$ with peaks at ~$Åk_{20}$ and ~$Åk_{40}$. SH-1 melilite does not show any distinct zoning features (Fig. 3), except for very gehlenitic melilite ($Åk_5$ to $Åk_{10}$) at the outermost edge of the CAI.

Fassaite in B1s studied here contains 8–14 wt% MgO and 12–24 wt% Al_2O_3 without any systematic differences between core and mantle unlike observed in [6].

Melilite in AL3529-26 appears as: (1) a layer of ~50–

60 μm grains in a ~100–150 μm thick rim together with anorthite, fassaite and spinel; (2) several blocky crystals; and (3) large irregular grains with intergrowth of pyroxene and anorthite. Melilite from the rim is very gehlenitic ($Åk_{5–30}$, peak at $Åk_{12–14}$) and mostly reversely zoned. Blocky melilite crystals in the central parts of the inclusion are normally zoned with composition varying from $Åk_{10}$ to $Åk_{70}$ with distinct peaks at $Åk_{36}$, $Åk_{46}$ and $Åk_{64}$. The majority of the melilite, however, exhibits patchy zoning. This melilite has the same range of compositions as the blocky ones but a single peak at $Åk_{36–38}$.

Fassaite from the interior of the inclusion AL3529-26 is very similar to that from other inclusions studied here. The grains from the outermost rim of AL3529-26 are Ti-rich (up to 18 wt%) which is typical for fassaite from the melilite mantles of B1s, but not for B2s [6].

Comparison of natural and synthetic samples and conclusions: The results presented above obtained from detailed quantitative X-ray maps show that the range of melilite composition is essentially the same, with both gehlenitic ($Åk_{10}$) and åkermanitic ($Åk_{70}$) melilite being common in all CAIs studied here, regardless of weather they have well developed thick or only thin and incomplete melilite mantle. Except for inclusion SH-1, melilite of the outer parts of the CAIs is depleted in Mg and Si (more gehlenitic) then melilite from the interiors. The same features are also typical for melilite crystallized from CMAS liquids under extremely reducing conditions in the laboratory. These samples are also characterized by more gehlenitic melilite mantle forming at higher temperatures and irregularly distributed åkermanitic melilite in the interior where it appears with low temperature pyroxene and anorthite. Unlike natural CAIs, where melilite quite often appears as laths, melilite from the synthetic samples mostly crystallizes as blocky crystals. This difference might be caused by the small size (typically 2–2.5 mm) of the experimental charges and by compositional differences of the starting materials.

Quantitative mapping of melilite shows that even synthetic samples which experienced a simple one stage crystallization event can exhibit quite complex zoning patterns. Fig. 4 shows one such example from a sample cooled from 1380º to 1250ºC in H_2 at 2ºC/hr. Depending on the chosen profile through the melilite crystal, one would see normal zoning (1), no zoning until the end of the profile (2) or very irregular zoning (3). As expected, melilites from natural CAIs have even more complex zoning patterns. Therefore, any conclusions made based on zoning patterns of melilite alone should be considered with caution.

References. [1] Stolper E. and Paque J.M. (1986) *GCA*, *50*, 1785. [2] Mendybaev R.A. et al. (2006) *GCA*, *70*, 2622. [3] Richter F.M. et al. (2006) *Meteoritics*, *41*, 83. [4] Murray J. et al. (2003) *LPS XXXIV*, #1999. [5] Caillet C. et al. (1986) *GCA*, *57*, 4725. [6] Simon S.B. and Grossman L. (2006) *GCA*, *70*, 780.

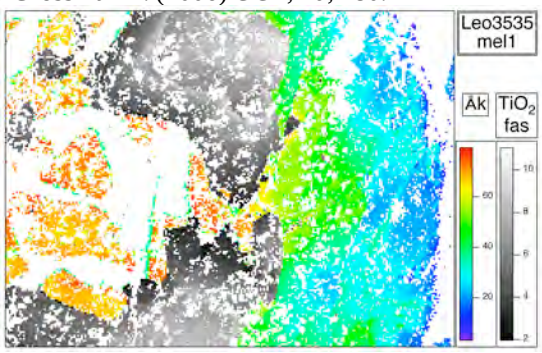

Fig. 1. Melilite composition map of the mantle of Leo3535.

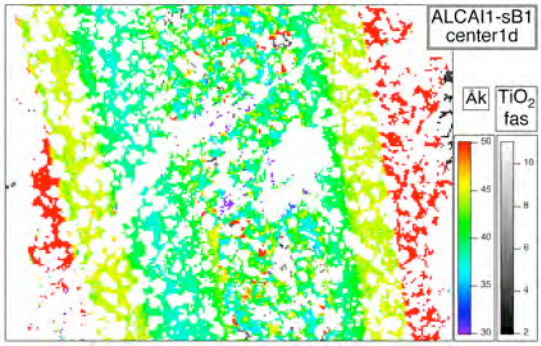

Fig. 2. Composition map of melilite lath from ALCAI1-sB1.

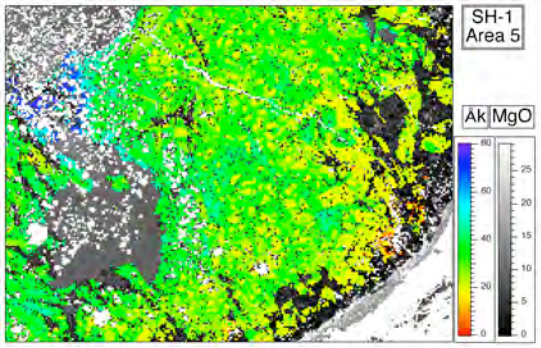

Fig. 3 Melilite composition map of the mantle of SH-1.

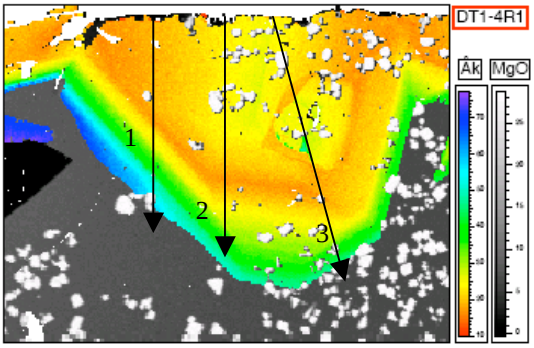

Fig. 4. Composition map of melilite crystallized by cooling of CMAS liquid in H_2 from 1380º to 1250ºC at 2ºC/hr. Linear profiles taken through the melilite grain would show different zoning patterns.